Archive for Organic Chemistry

The Free Internet Journal for Organic Chemistry

Paper

Arkivoc **2020**, part ii, 102-112

Carbocation inside the cage: a periodical DFT study on the interaction of the $C_4H_7^+$ system with alkali metal ion-exchanged zeolite Y

Nilton Rosenbach Jr[a]. and Claudio J. A. Mota[b,c]

[a]*Centro Universitário Estadual da Zona Oeste. Avenida Manuel Caldeira de Alvarenga, 1203, 23070-200, Campo Grande, Rio de Janeiro, Brazil*

[b]*Universidade Federal do Rio de Janeiro, Instituto de Química. Av Athos da Silveira Ramos 149, CT Bl A. Rio de Janeiro, 21941-909, Brazil*

[c]*Universidade Federal do Rio de Janeiro, Escola de Química. Av Athos da Silveira Ramos 149, CT Bl E. Rio de Janeiro, 21941-909, Brazil*

Email: cmota@ig.ufrj.br

Received 11-16-2019 **Accepted** 03-30-2020 **Published on line** 04-03-2020

Abstract

Periodic DFT calculations at GGA-PPBE level were carried out with the goal of achieving better understanding of the influence of the polarity of the zeolite cavity on the stability of carbocations intermediates inside these materials. The results show that local electrostatic interactions play the major role of stabilizing such species on the zeolite surface.

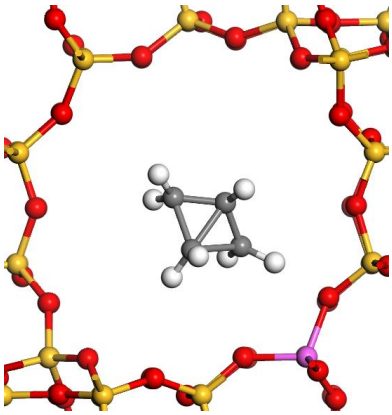

Keywords: Zoelite, bicyclobutonium, periodical DFT calculations, solid solvent

Introduction

Zeolites are porous aluminosilicates widely used as catalysts in the petrochemical industry, mainly because of their activity and selectivity in processes such as cracking, isomerization and alkylation. Based on the similarities with superacid media,[1] most of the initial studies suggested that carbocations were the key intermediates in zeolite-catalysed hydrocarbon transformations. In such process, zeolites act as Bronsted acids, transferring a proton to the hydrocarbon to yield ionic intermediates. However, simple carbocationic species are seldom observed on the zeolite surface as long-living species as observed, for instance, in superacid media. In fact, only some conjugated cyclic carbocations are both, experimental and theoretically, characterized as persistent species. Hence, covalent species, namely alkoxides[2] (Figure 1), are thermodynamically more stable than simple alkyl carbocation,[3,4] and are observed as persistent intermediates on the zeolite surface. Some of these studies suggested that alkoxides were the real intermediates involved in hydrocarbon reactions over zeolites, whereas carbocations were just transition states on these reactions.[5–7]

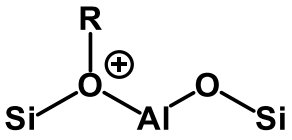

Figure 1. Pictorial Representation of the Alkoxide on the Zeolite Surface.

We have been studying the nature of carbocations adsorbed on the zeolite surface employing metal-exchanged zeolite and alkylhalides.[8–10] In these systems, the metal cation acts as a Lewis acid site, coordinating with the alkylhalide to form a metal-halide species and a carbocation inside the zeolite cavity. We were able to show the rearrangement of cyclopropylcarbinyl chloride over NaY at room temperature.[11] Similar to what takes place in solution, we interpreted the results in terms of formation of a bicyclobutonium cation ($C_4H_7^+$), which may be nucleophilic attacked in three different positions, giving rise to cyclobutyl and allylcarbinyl halides, as well as the parent cyclopropylcarbinyl, as depicted in the Figure 2.

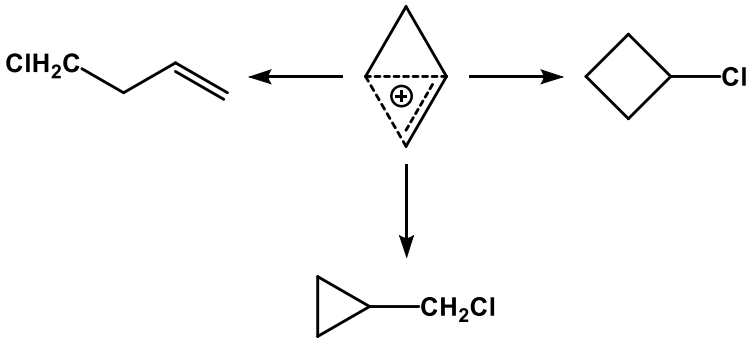

Figure 2. Product distribution of nucleophilic attack on the three-centre bond of the bicyclobutonium cation.

We also carried out the reaction of cyclopropylcarbinyl chloride with NaY impregnated with NaBr. Besides the rearranged chlorides, we were able to observe cyclopropyl, cyclobutyl and allylcarbinyl bromides, formed upon the nucleophilic attack of the impregnated bromide ion to the bicyclobutonium cation (figure 3). In addition, we were able to observe an unknown nucleophilic substitution process, named halogen switch

reaction (HSR). This reaction takes place when passing a mixture of alkyl halides (bromide and chloride) with different alkyl structure over the zeolite. Upon passing an equimolar mixture of cyclopropylcarbinyl chloride and *tert*-butyl bromide over NaY at room temperature, we observed the formation of cyclopropyl, cyclobutyl and allylcarbinyl bromides, as well as tert-butyl chloride.

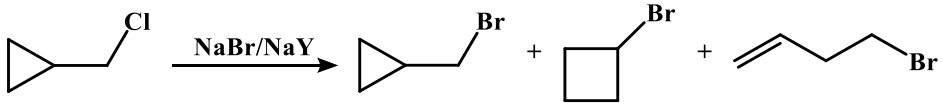

Figure 3. Rearrangement and nucleophilic substitution of cyclopropylcarbinyl chloride over NaY zeolite impregnated with NaBr.

The experimental results were supported by DFT calculations, which also revealed that bicyclobutonium cation is formed within the pores of zeolite Y as a minimum in the potential energy surface. According to these calculations, the cyclopropyl, cyclobutyl and allylcarbinyl alkoxides are the most stable species, which explains the spectroscopic results that point out the alkoxides as the long-living species on the zeolite surface. However, DFT molecular dynamics simulations of the $C_4H_7^+$ system, within the pores of zeolite Chabazite at different temperatures, showed that the alkoxides are formed only when the bicyclobutonium cation is favourably orientated near the framework oxygen atom.[12] Increasing the temperature induces carbocation mobility towards the centre of the cavity and reduces the chances for the formation of the alkoxide. Nevertheless, when the alkoxide is formed it persists for a long period.

The experimental and theoretical results are unequivocal evidences for the ionization of alkyl halides within the pores of zeolites to form simple alkyl carbocations as discrete intermediates. We proposed that zeolites might behave as solid solvents, inducing ionization of the substrate and stabilization of the ionic species formed, similarly to what takes place in solution, in which the solvent molecules surround ionogen molecules to stabilize intermediates and transition states. Although this concept has already been introduced by Derouane, he emphasized the confinement effects which stem from long-range attractive van der Waals interactions and would be responsible for all the catalytic properties of zeolites.[13] Although the dielectric constant of zeolites is small ($\varepsilon \approx 1.6$), the presence of cations such as Na^+, K^+, Mg^{2+}, and Ca^{2+}, located near trivalent cations such as Al^{3+}, induces large electrostatic fields.[14] It suggests that coulombic interactions can play a major role on the stabilization of ionic intermediates and transition states, rather than confinement effects. Actually, short-range interactions due to the presence of extra-framework aluminum species (EFAL) might explain why HUSY provides the most energetically favourable environment for the formation of bicyclobutonium cation from ionization of cyclopropylcarbinyl chloride as we have recently shown.[15] Some EFAL species, which have ionic nature, may increase the local polarity and induce ionic reactions.[16]

In order to investigate such effect in more detail, we report here a DFT calculations using periodic boundary conditions (PBC) to investigate the stability of the $C_4H_7^+$ species within the pores of zeolite Y impregnated with NaCl and NaBr.

Results and Discussion

The optimized structures of the bicyclobutonium and cyclopropylcarbinyl carbocations on the pure zeolite Y (without impregnation of the metal halides) are similar to that calculated employing the ONIOM scheme, at

PBE1PBE/6-31G(d,p):MNDO level.[11] Although the distance between both carbocations and the zeolite Y surface is slightly longer at the theoretical level used here, the $C_4H_7^+$ species are still located near the framework and may be stabilized by hydrogen bonding with the oxygen atoms of the zeolite structure. We did not explore all minima for the bicyclobutonium inside the zeolite Y pore network, since our main goal in this work is to investigate the effect of impregnation of metal halides on the stability of the carbocations.

Table 1 shows the relative stability of the $C_4H_7^+$ species on zeolites Y and Chabazite. All the alkoxides are more stable than the bicyclobutonium and cyclopropylcarbinyl cations. Cyclopropylcarbinyl and cyclobutyl alkoxides are slightly less stable (2.4 and 4.4 kcal.mol^{-1}, respectively) than allylcarbinyl alkoxide. These results are in agreement with the thermodynamic stability of the respective chlorides at the same level of theory, as well as with previous calculations of the $C_4H_7^+$ species on Chabazite.[12] On the other hand, the energy difference between the carbocations and the allylcarbinyl alkoxide is smaller within the Chabazite cage than in zeolite Y. This might reflect the stronger steric repulsion betweem the alkoxide and the zeolite framework on zeolites of more constrained pore environment. In fact, Chabazite consists of a network of hexagonal prisms connected by four-membered rings with ellipsoidal cavities of 8.4 Å, whereas zeolite Y presents cavitie with pore diameter of 12.4 Å.

Table 1. Relative energy (values in kcal mol^{-1}) among $C_4H_7^+$ species on zeolites Y and Chabazite[12] calculated at GGA-PPBE level with D3 vdW corrections

Specie	Zeolite Y	Zeolite Chabazite
Cyclobutyl alkoxide	5.7	-
Cyclopropylcarbinyl alkoxide	3.8	-
Allylcarbinyl alkoxide	0.0	0.0
Bicyclobutonium cation	22.8	16.8
Cyclopropylcarbinyl cation	23.9	18.2

The ionization of cyclopropylcarbinyl chloride/bromine on the zeolite Y surface is preceded by its physisorption. The optimised structures of the adsorption complex show an ion–dipole interaction between the halogen atom and the cation, which does not significantly disturb the sodium/lithium position as shown in Figure 4 for cyclopropylcarbinyl chloride adsorbed on NaY. The halogen atom of the cyclopropylcarbinyl halides pull the sodium/lithium ion out from its starting position, slightly stretching the Li or Na-O(zeolite) distances.

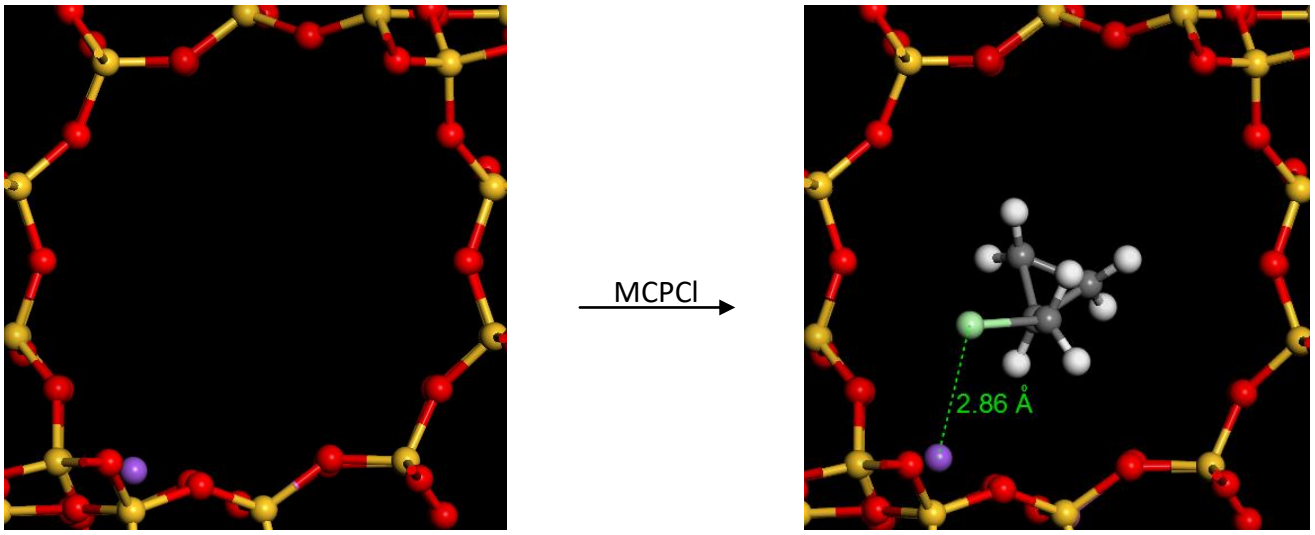

Figure 4. Optimized structures; (a) model of NaY and (b) cyclopropylcarbinyl chloride (MCPCl) adsorbed on NaY, calculated at GGA-PPBE level (O atoms in red, Si atoms in yellow, Al atom in purple, Cl atom in green, Na atom in purple, H atoms in white and carbon atoms in grey).

Table 2 shows the Li^+ and Na^+ halide distances for the adsorption complex of cyclopropylcarbinyl chloride/bromine on the zeolite surface. The order reflects the strength of the ion-dipole interaction. The smaller and more polarized halide atom undergoes a stronger electrostatic interaction with the smaller and more polarized cation. Thus, the stronger interaction occurs between Li^+ and chloride, whereas Na^+ and bromide shows the weakest ion-dipole interactions. Table 2 also shows that formation of all adsorption complexes are exothermic compared to the isolated reactants and reflects the strength of the ion-dipole interaction. Dispersive interactions play a significant role on the physisorption process, because adsorption energy increases almost by a factor of two when D3 vdW corrections are included in the calculations.

Table 2. Energetics (values in kcal mol^{-1}) and M-X distances (values in angstrom) for the adsorption of cyclopropylcarbinyl chloride/bromine on the metal-exchanged zeolite Y (MY, M=Li or Na) calculated at GGA-PPBE level with D3 vdW corrections (bracketed values does not include D3 vdW corrections)[a]

Cyclopropylcarbinyl	MY		M-X distance	
halide	LiY	NaY	Li	Na
Chloride	-29.5 (-18.2)	-29.2 (-16.8)	2.434	2.860
Bromine	-27.3 (-15.9)	-27.7 (-15.3)	2.614	2.959

[a] relative to the isolated cyclopropylcarbinyl halide and LiY or NaY.

The optimized structures of the bicyclobutonium cation and allylcarbinyl alkoxide on the zeolite Y impregnated with NaCl are shown in Figure 5. The geometries of all the others $C_4H_7^+$ species adsorbed on the zeolite Y impregnated with LiCl, LiBr and NaBr are similar.

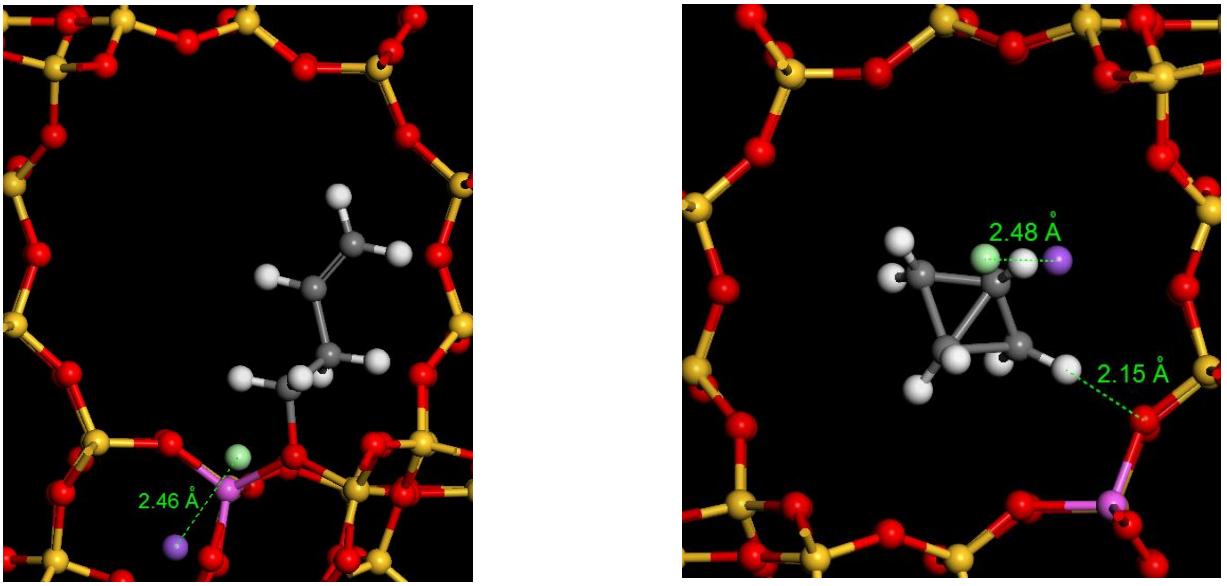

(a) (b)

Figure 5. Optimized structures of (a) allylcarbinyl alkoxide and (b) bicyclobutonium cation adsorbed on zeolite Y impregnated with NaCl and calculated at GGA-PPBE level (O atoms in red, Si atoms in yellow, Al atom in purple, Cl atom in green, Na atom in purple, H atoms in white and carbon atoms in grey).

After ionization, the position of the sodium or lithium cation is significantly disturbed by interactions with chlorine or bromine anions for all geometries of the bicyclobutonium cation considered in the initial screening. The presence of both anions induces cation mobility towards the centre of the super-cage near the $C_4H_7^+$ species to interact with the halide. However, such interactions do not lead to significant change in the position of the ions, compared with the geometry of the bicyclobutonium cation and alkoxide structures, allowing us to assess the relative stability of all $C_4H_7^+$ species and capture only the stabilizing effect due to the presence of the MX unit. It might be also emphasized that the position of some extra-framework cations for the same system remains uncertain, especially for those occupying low symmetry sites with low occupancy factors.[17] Table 3 shows the M-X distance in the presence of the bicyclobutonium cation and the allylcarbinyl alkoxide. Although the difference is small compared to the allylcarbinyl alkoxide, the MX distance is slightly streched when the monomer unit lies in the presence of the bicyclobutonium cation, due to the stronger interaction between the halide and the $C_4H_7^+$ cation. Such trend may reflect some degree of interaction between the MX unit, the bicyclobutonium cation and the zeolite Y framework, because in the presence of the cation or the alkoxide, the MX distance are slightly stretched when compared with experimental data.

Table 3. M-X distance (values in angstrom) for the MX unit in the presence of the bicyclobutonium cation and the allylcarbinyl alkoxide on the zeolite Y, calculated at GGA-PPBE level

M-X distance	Bicyclobutonium cation	Allylcarbinyl alkoxide	Experimental*
Li-Cl	2.155	2.134	2.021
Li-Br	2.316	2.296	2.170
Na-Cl	2.482	2.459	2.361
Na-Br	2.631	2.613	2.502

* Values for the MX unit available at NIST Chemistry WebBook.[18]

Table 4 shows the relative stability of the $C_4H_7^+$ species on the zeolite Y impregnated with LiCl, LiBr, NaCl and NaBr. The presence of all monomeric species (MX) significantly increases the stability of the bicyclobutonium cation, reducing the energy difference between the cation and the allylcarbinyl alkoxide in approximately 10 kcal mol^{-1}, when compared with $C_4H_7^+$ species adsorbed on the pure zeolite Y (without the impregnated MX unit). Such effect is more pronounced on zeolite Y impregnated with lithium chloride, whereas stabilization of the bicyclobutonium cation is lower in the presence of sodium bromide. The relative stability does not change significantly if the D3 vdW corrections are included in the calculations.

Table 4. Energy difference (values in kcal mol^{-1}) among $C_4H_7^+$ species on the zeolite Y surface impregnated with LiCl, LiBr, NaCl and NaBr calculated GGA-PPBE level with D3 vdW corrections (bracketed values does not include D3 vdW corrections)

Specie	LiCl	LiBr	NaCl	NaBr
Cyclobutyl alkoxide	5.7 (4.0)	6.0 (4.2)	6.9 (4.4)	6.7 (4.3)
Cyclopropylcarbinyl alkoxide	4.1 (2.3)	4.2 (2.4)	4.7 (2.4)	4.8 (2.5)
Allylcarbinyl alkoxide	0.0 (0.0)	0.0 (0.0)	0.0 (0.0)	0.0 (0.0)
Bicyclobutonium cation	12.6 (10.8)	12.9 (11.1)	13.9 (11.5)	14.5 (12.1)

In order to investigate the degree of stabilization of carbocations and alkoxides due to short-range electrostatic interactions, we introduce another NaCl unit in the zeolite Y cage. The energy difference between the bicyclobutonium carbocation and the allylcarbinyl alkoxide decrease further as shown in the Figure 6.

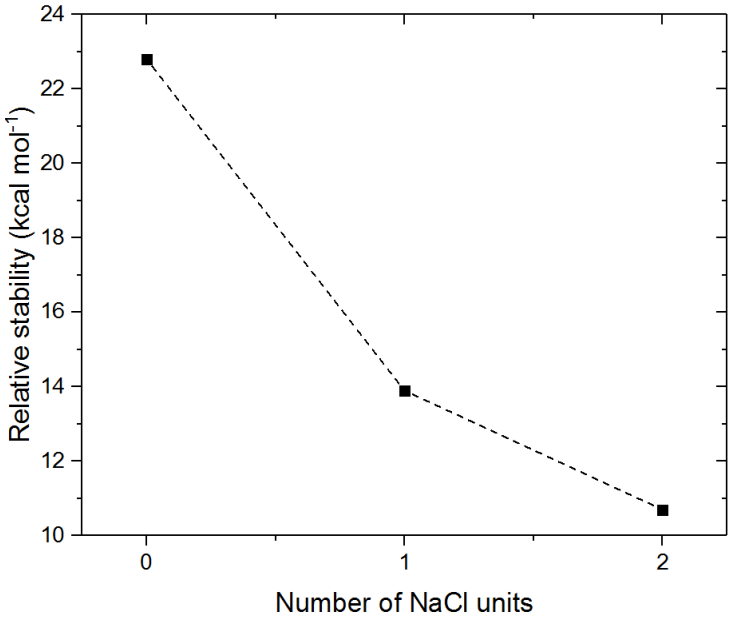

Figure 6. Energy difference (values in kcal mol^{-1}) between the bicyclobutonium carbocation and the allylcarbinyl alkoxide on the zeolite Y impregnated with NaCl, calculated at GGA-PPBE level with D3 vdW corrections.

These results reinforce the idea that carbocations might be in equilibrium with the alkoxides within the zeolite cavities. Increasing the polarity of the zeolite environment, due to the presence of impregnated ionic species, contributes to the stabilization of the carbocations. Short-range electrostatic interactions may play a major role in stabilizing such species.

Dispersion interactions requires a more appropriate treatment than that given by standard DFT methods. In fact, adsorption of C_2H_2 on NaCl(001) surface is in fair agreement with experimental data if dispersion interactions of the Grimme D3 type are included in the treatment.[19] The results reinforce such effect mainly in the physisorption process and suggest that the interaction between the bicyclobutonium cation and the MX species within the zeolite Y cage is essentially electrostatic, hence the dispersion interactions play a minor role in the stabilization of the cationic species.

Conclusions

Periodical DFT calculations showed that the stability of the bicyclobutonium cation within zeolite Y cavity increases in the presence of ionic species such as LiCl, LiBr, NaCl and NaBr, when compared to the allylcarbinyl alkoxide. The degree of stabilization depends on the polarity of the zeolite environment and increases further when another NaCl unit is introduced in the cavity.

These results reinforce the hypothesis that zeolites behave as solid solvents in which short-range interactions, such as hydrogen bonds and electrostatic forces, play a more significant role in stabilizing ionic species rather than long-range van der Waals interactions. It may change the way zeolite catalysts are designed by shifting the focus from increasing the acid strength to structural or pore environment modifications that yield materials able of stabilizing intermediates and transition state with ionic character.

Computational Methods

The calculations were carried out with a primitive rhombohedral unit cell of zeolite Y (a=b=c=17.75 Å α=β=γ=60°) containing 144 atoms ($Si_{48}O_{96}$). All silicon atoms are equivalent and there are four oxygen atoms crystallographically distinct labeled O_n. In this structure, sodalite units are connected by hexagonal prisms forming cavities with pore diameter of 12.4 Å. A silicon atom was isomorphically replaced by an aluminum atom so the Si/Al ratio is 47. The Al atom charge was adjusted by introducing ionic or covalent species near the aluminum atom. The bicyclobutonium cation was embedded by hand in the main channel near the aluminum atom while the alkoxides were introduced in the oxygen position O_1 bound to the Al site. Such position is projected towards the supercavity and therefore, it is more accessible to reactant molecules. In those models of the zeolite Y impregnated with LiCl, LiBr, NaCl and NaBr, the cations were introduced in the six-membered rings of the sodalite cage labeled site II. Such site is preferentially occupied by lithium and sodium ions according to most studies.[20] We did not take into account the influence of the adsorbent species on the unit cell volume. In such molecular model, the shortest distance between atoms from reactive domain and their repeated images is greater than 17 Å, which decreases undesired interactions, as other studies involving similar systems have shown.[21]

DFT calculations using pseudopotentials to describe ion cores and plane-wave basis sets were performed with Quantum-Espresso package.[22] All atoms were described by the generalized gradient approximation GGA-PBE for the exchange correlation functional[23] along with Vanderbilt ultrasoft pseudopotentials[24] to describe the ion cores. The energy cutoff was set to 50 Ry and the electron density was obtained at the Γ point in the first Brillouin zone. The atomic positions were relaxed until all the force components on each atom were less than 0.001 Ry/Bohr and the convergence criterion of 10^{-4} Ry was reached for the total energy. In order to describe accurately

Dispersion interactions, not included in the GGA-PBE functional, were taken into account using D3 method developed by Grimme, in which the van der Waals interactions are described as an atom-pairwise correction with more accurate C_6 coefficients that improve description of large (periodic) systems.[25] DFT-3 corrections were perfomed in single point calculations of the optimized geometry and added to the pure GGA-PBE final energy.

Acknowledgements

We thank CNPq, CAPES and FAPERJ for financial support.

References

1. Olah, G. A. ; Prakash, G. K. S. ; Sommer, J. *Superacid Chemistry*, Wiley-Interscience: New York, 1985.
2. Haw, J. F.; Nicholas, J. B.; Xu, T.; Beck, L. W.; Ferguson, D. B. *Acc. Chem. Res.* **1996**, *29* (6). https://doi.org/10.1021/ar950105k.
3. Haw, J. F.; Richardson, B. R.; Oshiro, I. S.; Lazo, N. D.; Speed, J. A. *J. Am. Chem. Soc.* **1989**, *111* (6), 2052–2058. https://doi.org/10.1021/ja00188a016.

4. Aronson, M. T.; Gorte, R. J.; Farneth, W. E.; White, D. *J. Am. Chem. Soc.* **1989**, *111* (3), 840–846. https://doi.org/10.1021/ja00185a009.
5. Kazansky, V. B.; Frash, M. V.; Van Santen, R. A. *Catal. Letters* **1997**, *48* (1–2), 61–67. https://doi.org/10.1023/A:1019066718512.
6. Viruela-Martin, P.; Zicovich-Wilson, C. M.; Corma, A. *J. Phys. Chem.* **1993**, *97* (51), 13713–13719. https://doi.org/10.1021/j100153a047.
7. Kazansky, V. B. *Acc. Chem. Res.* **1991**, *24* (12), 379–383. https://doi.org/10.1021/ar00012a004.
8. Correa, R. J.; Mota, C. J. *A. Appl. Catal. A Gen.* **2003**, *255* (2), 255–264. https://doi.org/10.1016/S0926-860X(03)00568-4.
9. Corrêa, R. J.; Mota, C. J. A. *Phys. Chem. Chem. Phys.* **2002**, *4* (17), 4268–4274. https://doi.org/10.1039/b200458e.
10. Rosenbach, N.; dos Santos, A. P. a.; Franco, M.; Mota, C. J. A. *Chem. Phys. Lett.* **2010**, *485* (1–3), 124–128. https://doi.org/10.1016/j.cplett.2009.12.003.
11. Franco, M.; Rosenbach, N.; Ferreira, G. B.; Guerra, A. C. O.; Kover, W. B.; Turci, C. C.; Mota, C. J. A. *J. Am. Chem. Soc.* **2008**, *130* (5), 1592–1600. https://doi.org/10.1021/ja0742939.
12. Kling, D. P.; Machado, E. S. A.; Chagas, H. C.; Dos Santos, A. P. A.; Rosenbach, N.; Walkimar Carneiro, J.; Mota, C. J. A. *Chem. Commun.* **2013**, *49* (40), 4480–4482. https://doi.org/10.1039/c3cc40627j.
13. Derouane, E. G. *Journal of Molecular Catalysis A: Chemical*, 1998; Vol. 134, pp 29–45. https://doi.org/10.1016/S1381-1169(98)00021-1.
14. van Santen, R. A.; Kramer, G. *J. Chem. Rev.* **1995**, *95* (3), 637–660. https://doi.org/10.1021/cr00035a008.
15. Arca, H. A.; Mota, C. J. A. *Top. Catal.* **2018**, *61* (7–8), 616–622. https://doi.org/10.1007/s11244-018-0911-8.
16. Bhering, D. L.; Ramírez-Solís, A.; Mota, C. J. A. *J. Phys. Chem. B* **2003**, *107* (18), 4342–4347. https://doi.org/10.1021/jp022331z.
17. Buttefey, S.; Boutin, A.; Mellot-Draznieks, C.; Fuchs, A. H. *J. Phys. Chem. B* **2001**, *105* (39), 9569–9575. https://doi.org/10.1021/jp0105903.
18. Lemmon, E. W.; McLinden, M. O.; Friend, and D. G. *NIST Chemistry WebBook,* 2017. https://doi.org/10.18434/T4D303.
19. Ehrlich, S.; Moellmann, J.; Reckien, W.; Bredow, T.; Grimme, S. *Chemphyschem* **2011**, *12* (17), 3414–3420. https://doi.org/10.1002/cphc.201100521.
20. Frising, T.; Leflaive, P. *Microporous Mesoporous Mater.* **2008**, *114* (1–3), 27–63. https://doi.org/10.1016/j.micromeso.2007.12.024.
21. Nieminen, V.; Sierka, M.; Murzin, D. Y.; Sauer, J. *J. Catal.* **2005**, *231* (2), 393–404. https://doi.org/10.1016/j.jcat.2005.01.035.
22. Giannozzi, P.; Baroni, S.; Bonini, N.; Calandra, M.; Car, R.; Cavazzoni, C.; Ceresoli, D.; Chiarotti, G. L.; Cococcioni, M.; Dabo, I.; et al. *J. Phys. Condens. Matter* **2009**, *21* (39). https://doi.org/10.1088/0953-8984/21/39/395502.
23. Perdew, J. P.; Wang, Y. *Phys. Rev. B* **1992**, *45* (23), 13244–13249. https://doi.org/10.1103/PhysRevB.45.13244.
24. Vanderbilt, D. *Phys. Rev. B* **1990**, 41 (11), 7892–7895.

https://doi.org/10.1103/PhysRevB.41.7892.
25. Grimme, S.; Antony, J.; Ehrlich, S.; Krieg, H. *J. Chem. Phys.* **2010**, *132* (15), 154104. https://doi.org/10.1063/1.3382344.